Validation of a Computer Aided Segmentation System for Retinography

Validation of a Computer Aided Segmentation System for Retinography

M. Baroni[1], P. Fortunato[2], L. Pollazzi[2], and A. La Torre[2]

[1] Dept of Information Engineering, University of Florence, Italy
[2] Dept of Oto-Neuro-Ophthalmological Surgical Sciences, University of Florence, Italy

Abstract—**In spite of the huge literature on angiography, some problems are still open to discussion, such as segmentation of entire vascular networks. In the present work a new computer approach is developed in two stages, with the aim of improving the analysis and comparison of retina vessel images in the follow up of patients. The first stage adopts multiscale filtering to detect objects of different sizes: a two scale Laplacian of Gaussian scheme is used with the related sigma values chosen according to the smallest and greatest vessel widths. An approximate segmentation is achieved simply by means of the Laplacian sign. The interpretation stage is application-specific and accomplishes classification and quantitative analysis. The skeleton of the binary structures is subdivided in vessel segments, their features (intensity, position, length and width) are fed into an artificial neural network (ANN), after back-propagation training. The segments classified as vessels are assembled into the retinal vascular tree by rule-based tracking, starting from optic disc (OD). Results are evaluated on STARE and DRIVE data bases. Accuracy is 95% and the false positive rate is decreased to about 1%, lower than literature values.**

Keywords—**angiography, retina, vessel segmentation, artificial neural network, tracking.**

I. INTRODUCTION

Many pathologies may affect blood vessels in all the body districts, which can be investigated by a wide range of angiographic modalities. Accordingly, many computer methods [1] have been developed to support medical research and routine examinations and to improve visual inspection of angiograms. The first step of these methods is segmentation: vessels are detected from a structured and noisy background. Then, vessel features are measured, such as width, length, branching angles and tortuosity [2]. Unfortunately, computer segmentation is not always fully automatic nor it warrant optimal performances. Accuracy depends on image quality: acquisition and pathological artifacts can not be always distinguished by blood vessels, so the analysis results are biased by the false positive rate.

Our specific interest regards retinal vessels that can be observed directly and non-invasively with color fundus photos, i.e. their green channel that has the best contrast. A computer vision approach detects candidate vessels with multiscale filtering, splits them into segments, that are then classified by a trained ANN and tracked from optic nerve heads (OD), so as to reduce false positives. The proposed approach is validated with STARE [3] and DRIVE [4] retinal databases, as they also provide vessel segmentation by two observers.

II. METHODS

A. Image Pre-processing and Segmentation

Among previous vessel segmentation methods, here we refer to matched filters [3], classification of Gaussian [4] or Wavelet featutres [5] or to their adaptive thresholding [6].

In this work, retinal images have been enhanced by Laplacian of Gaussian (LoG) filtering, implemented in its fast, separable form, as mono-dimensional convolutions (indicated with *, instead of 2D convolution ⊗), according to Marr & Hildreth:

$$LoG(x,y) = \frac{\partial^2}{\partial x^2}[I(x,y) \otimes G(x,y)] + \frac{\partial^2}{\partial y^2}[I(x,y) \otimes G(x,y)] =$$

$$= G(x) * [I(x,y) * \frac{\partial^2}{\partial y^2} G(y)] + G(y) * [I(x,y) * \frac{\partial^2}{\partial x^2} G(x)]$$

where I(x,y) is the image to be processed and G(x) or G(y) are 1D Gaussian functions, defined as follows:

$$G(x) = \frac{1}{\sqrt{2\pi\sigma^2}} \exp(\frac{-x^2}{2\sigma^2})$$

Gaussian filters can be tuned by varying the sigma parameter and they respond to vessels as well as to spurious objects, so that the extracted features should be examined by a subsequent classifier. On the other hand, vessel width varies from tens of pixels to sub-pixel level. It is well known how such filters preserve the objects of size tuned to their scale, whereas other objects are smoothed and smeared, till to cancel the finest ones.

Therefore, multiscale filtering has been adopted to simulate the visual perception of human observers: edges are detected at a coarse scale and then are localized at the finest scale. The greater and smaller sigma values have been chosen according to the expected maximal and minimal vessel width, respectively. The outputs of LoG filters with these scale values are very similar to the response of a Gaussian matched filter, because they extract the whole vessel width. Using smaller sigma values, or applying these values to larger vessels, results in extracting the edges of vessels rather than whole vessels. Two dimensional Laplacian changes sign across boundaries and therefore

L.M. Roa Romero (ed.), *XIII Mediterranean Conference on Medical and Biological Engineering and Computing 2013*, IFMBE Proceedings 41,
DOI: 10.1007/978-3-319-00846-2_67,

segmentation is achieved by a unique threshold: pixels with negative Laplacian are marked as vessels (white), and the other pixels as background (black).

A novel scheme is used to combine the two scale outputs: a bit-wise AND is operated at pixel level, between the thresholded coarse and fine scale Laplacian images. In this way, the small vessels that are detected also at the coarse scale, preserve their original width, whereas the noisy structures detected only at the fine scale are canceled. As a possible drawback of this scheme, larger vessels may exhibit spurious holes, where their width is over the filter scale. To avoid this and other artifacts in the subsequent skeletonizing step, simple median filtering is used, as a cleaning procedure on the segmented images, according to the following sequence:

$$I_r = [\ (I_{\sigma 1} \otimes m_5) \cap \ I_{\sigma 2}\ ] \otimes m_3$$

where I_r is the resulting segmented image, $I_{\sigma 1}$ and $I_{\sigma 2}$ are the binary fine and coarse scale Laplacian images, which are combined by means of a pixel-by-pixel AND operator; finally, m_5 and m_3 indicate median filters, with 5x5 and 3x3 windows, respectively.

Then, a classical thinning algorithm is used to extract the skeleton of the low level vascular tree. Thinning deletes border points without destroying connectivity and its result is a connected, topological preserving central axis of the vascular tree. Three types of significant points are detected in the skeleton: terminal points, bifurcation points and crossing points. Based on these points, skeletons are partitioned into single segments. Two neighboring bifurcation points are merged into one crossing points [2].

B. Vessel Classification and Tracking

The candidate vessels, first extracted by the LoG sign, must then be classified. From experts' descriptions of vascular trees, the most relevant features for classification can be derived. Specifically, each skeleton vessel segment is tracked from an outermost point to the other one, by using a chain code, and the following measurements are made: length, width, inner and outer intensity, position with respect to the optic disc. This analysis module gives a length value, L (along the skeleton segment), and mean and s.d. values of width, Wm and Wsd (estimated at every three skeleton points as the shortest path across the binary vessel).

Moreover, an average value of inner intensity, I, is computed through region growing on the green image within each single binary region. To try a distinction between true vessels and false positives, also an outer intensity index, O, is evaluated as follows. The average gray level, O1 and O2, and their s.d. are computed for both the regions besides each candidate binary region, with equal length and half width. If $\delta=|O1-O2|>$ s.d., the outer intensity index, O, is set to $-\delta$, indicating a possible false positive (e.g. due to OD border, between the bright disc and the dark retinal background); otherwise O is set to (O1+O2)/2. This value indicates a possible true vessel or an artifact between two pathological structures (e.g. exudates) which can be discriminated when the latter are much brighter than normal retinal background. Finally, by using the two outermost points of each segment, two distances from OD, d1 and d2, are computed for each candidate vessel segment. To this aim, the brightest and greatest blob has been detected by smoothing the green images and by matching a 2D Gaussian to yield approximate locations of OD.

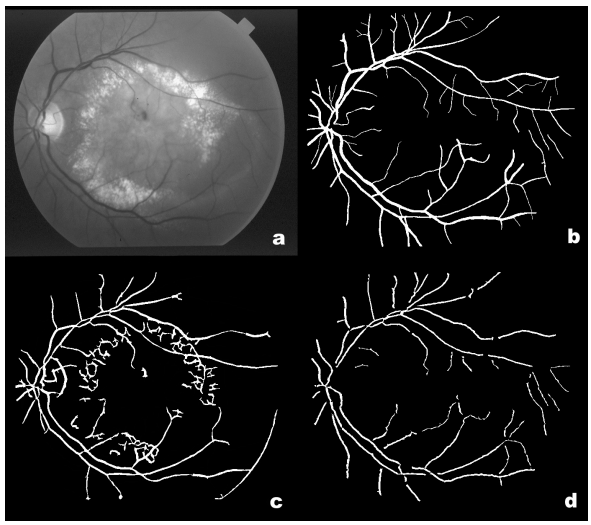

Fig. 1 a) Green channel of an abnormal fundus image of STARE database. b) manual segmentation. c) segmentation by the Hoover's method [3]. d) segmentation by the proposed method (LoG-ANN).

For each candidate vessel we have seven features that are fed into an artificial neural network (ANN) to make the classification. Among the various ANN classifiers, a three layers feed-forward architecture has been chosen and trained through the back-propagation algorithm. The input layer has seven neurons, according to the aforementioned feature vectors, and the output layer has one neuron. The number n of hidden layer neurons has been empirically determined, in order to maximize the mean square error during training and testing as well as to improve generalization. To the latter aim, the number of the vessel segments in the training set is taken greater than the number of parameters in the network.

The binary segments classified as vessels are then assembled into their vascular tree by a tracking algorithm: they are sorted based on the distance from the optic disc (OD) and tracked by chain code, starting from their terminal point nearer to OD. According to this distance sorting, the

vessel segments are labeled as roots (parents) of partial vessel trees. For each parent, its branches (daughters) are then tracked from the current bifurcation point till to another bifurcation point or till to their terminal point. The daughters of every parent vessel, v_k , are numbered as $2v_k$ and $2v_{k+1}$ in order to track the tree in either direction.

Tracking continues iteratively until no other daughters are detected and no other vessel segment has remained unlabeled and identified as a new parent. The final step of tracking examines again the labeled vessels, trying to connect them if their first terminal point (the terminal point nearer to OD) is within a short distance (r=20) from the second terminal point (the farther one from OD) of another labeled segment. This tracking is similar to [2] but it does not need user interaction and the r distance allows to follow interrupted vessels or disconnected branches, which may turn out from image artifacts due to processing or pathology. Finally, the vessel trees are filled from the labeled skeletons. From these vessel data, further geometrical and topological analysis may be accomplished.

III. EXPERIMENTAL EVALUATION AND RESULTS

Ad hoc software was written using a C++ programming environment and a neural network toolkit, developed beforehand at our lab. To devise the optimal settings of the proposed method, several experiments were undertaken. The best performance of Gaussian smoothing for optic disk (OD) matching was obtained with a sigma value of 5, whereas the smaller and greater sigma values for vessel segmentation have been chosen equal to 1 and 3, respectively. A human expert manually labeled the candidate vessel/nonvessel segments; their features were computed, normalized in the range [0,1], and fed into the ANN. The training set includes one half (10) of the STARE images and one half (20) of the DRIVE images. The other halves of both databases are included in the test set. The maximal number of epochs was 3000 and the goal mean square error was 0.005. The best network configuration has a number n = 20 of hidden layer neurons, and it was simulated with the test set for performance evaluation.

The STARE and DRIVE public databases provided a most valuable reference for these activities. Specifically, the proposed method is evaluated by computing sensitivity, specificity and accuracy at pixel level with respect to manually segmented vessels available in both databases. The first observer segmentation is taken as ground truth. Any pixel which is classified as vessel in both the ground truth and segmented image is accumulated among the true positives; any pixel classified as vessel in the segmented image but not in ground truth is counted among the false positives.

Illustrative segmentation results are shown in fig.1.

Table 1 presents the average values of specificity, sensitivity and accuracy computed on the DRIVE test images by different methods.

Table 1 Performance (%) of vessel segmentation (DRIVE database)

method	specificity	sensitivity	accuracy
2nd observer	97.25	77.61	94.73
Staal et al.[4]	97.73	71.94	94.42
Soares et al.[5]	97.88	72.83	94.66
Zhang et al.[6]	97.24	71.20	93.82
LoG-ANN	98.61	65.16.00	94.93

Table 2 Performance (%) of vessel segmentation (STARE database)

method	specificity	sensitivity	accuracy
2nd observer	93.90	89.49	93.54
Hoover et al.[3]	95.67	67.51	92.67
Staal et al.[4]	98.10	69.70	95.16
Soares et al.[5]	97.48	71.65	94.80
Zhang et al.[6]	97.53	71.77	94.84
LoG-ANN	98.72	63.06	94.78

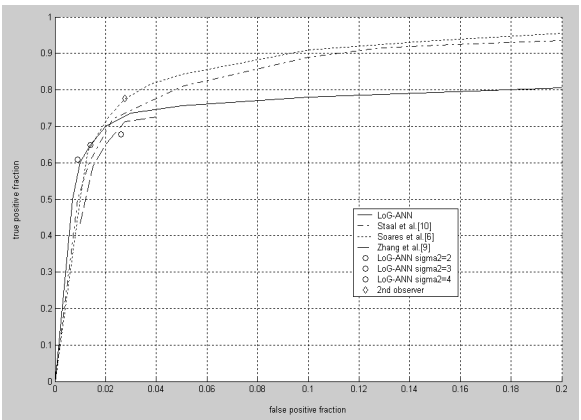

Fig. 2: The ROC curve for DRIVE database when False Positive Fraction is less than 0.2 for LoG-ANN, compared with three other published ROC curves and with manual segmentation. The circle markers refer to the best LoG-ANN results of multiscale filtering with the greater sigma value equal to 2, 3 or 4.

The same results of the appropriate methods applied to STARE database are presented in Table 2. Total accuracy, computed on both databases, was nearly 0.95 (0.9485 ± 0.003), which is comparable with the best accuracy values reported in literature. However, the false positive rate was

very close to 1%, so that specificity is better than 98%, whereas the values reported in literature are not better than 96 or 97 %. On the other hand, sensitivity is less than 70% and cannot reach the higher values reported in some papers (over 72% for [5,6], about 77% and 90% for the 2nd observer in DRIVE and STARE images respectively).

For a more complete comparison to previous works, ROC curves have been produced for both DRIVE and STARE databases by varying the sigma parameter of LoG filtering and the thresholds of the ANN results. The aforementioned performance values have been achieved by using the 0.5 value as the decision ANN threshold. At a threshold of 1 the false detection rate is zero, but no vessels are detected, while at a threshold of 0 all the candidate vessels are detected. Thus, this threshold is a natural choice to produce a ROC curve. Figure 2 and 3 show the ROC curves obtained by this and other methods [4-6] for test DRIVE and STARE images. To make the display clearer, results are shown for false positive fractions less than 0.2. Results for different values of the coarse-scale sigma parameter are shown only for 0.5 decision threshold. Varying the fine-scale sigma has not produced good results.

The performance of LoG-ANN method is similar to Zhang et al.[6]; it seems that these enhancement filters cannot detect all the vessels as segmented by the first observer. However, both ROC curves exhibit a portion higher than other methods. Finally, it is worth noting the optimal capability in discriminating between vessels and other spurious structures, as visible in pathological eyes (figure 1).

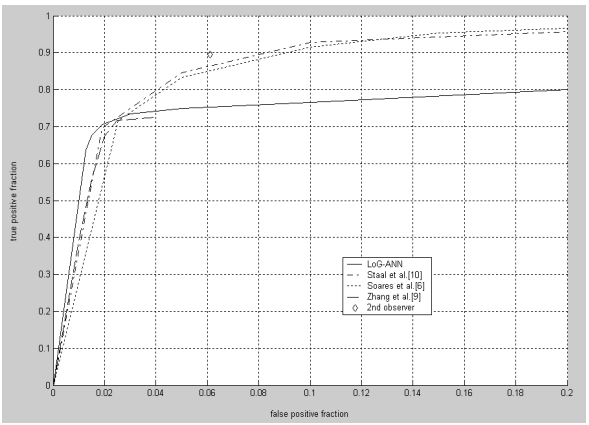

Fig. 3 The ROC curve for STARE database when FP < 0.2 for the proposed method (LoG-ANN) compared with three other published ROC curves and with the second observer's manual segmentation

IV. DISCUSSION

While the first stage of the proposed segmentation method detects candidate vessel segments, the second stage measures specific vessel features, recognizes them and reassembles the vascular tree. ANN classifier was chosen as it is robust and able to recognize simple vessel features. High sensitivity is not reached: however, a low false positive rate in vessel segmentation is very important in many applications. For example, in retinopathy of prematuriy, where therapy is decided according to normal or abnormal width and tortuosity of retinal vessels, it is essential to make these measurements on the whole length of principal vessels, whereas their thinner branches may give minor information.

In conclusion, though developed for retinal images, this method can be applied to other tree-like vascular images as soon as a starting point is detected.

REFERENCES

1. Fraza M, Remagninoa P, Hoppea A, et al. (2012) Blood vessel segmentation methodologies in retinal images–A survey. Computer Meth.&Progr.Biomed. 108: 407–433.
2. Martinez-Perez ME, Hughes AD, et al. (2002) Retinal Vascular Tree Morphology: A Semi-Automatic Quantification. IEEE Trans Biomed Eng. 49: 912-917.
3. Hoover A, Kouznetsova V, Goldbaum M. (2000) Locating blood vessels in retinal images by piecewise threshold probing of a matched filter response. IEEE Trans Med Imaging. 19:203–210.
4. Staal J, Abramoff MD, Niemeijer M, Viergever MA, van Ginneken B. (2004) Ridge-based vessel segmentation in color images for the retina. IEEE Trans Med Imaging. 23:501–509.
5. Soares JVB, Leandro JG, et al.(2006) Retinal Vessel Segmentation Using the 2-D Gabor Wavelet and Supervised Classification. IEEE Trans Med Imaging. 23:1214-1222.
6. Zhang B, Zhang L, Karray F. (2010) Retinal Vessel extraction by matched filter with first-order derivative of Gaussian. Computers in Biology and Medicine. 40:438–445.

Author: Maurizio Baroni
Institute: Dept of Information Engineering
Street: via Santa Marta 3
City: Firenze, 50139
Country: Italy
Email: maurizio.baroni@unifi.it